Intercalation in Zinc-Layered Hydroxide: Zinc Hydroxyheptanoate Used as Protective Material on Zinc

Emmanuel Rocca,* Celine Caillet, Adel Mesbah, Michel Francois, and Jean Steinmetz

Laboratoire de Chimie du Solide Minéral, UMR CNRS 7555, Université Henri Poincaré-Nancy I, BP 239, F-54506 Vandoeuvre-lès-Nancy Cedex, France

Received July 12, 2006. Revised Manuscript Received October 3, 2006

During transport or the storage, galvanized steel products undergo wet storage stain phenomenon, leading to the formation of an extensive white rust of zinc. The corrosion products are mainly zinc layered hydroxides salts of which allow several intercalation or coprecipitation reactions allowing the easy absorption of corrosive anions on the surface and then the corrosion of zinc. In the context of developing effective, low-cost, and environmentally friendly corrosion inhibitors, this study is focused on the action of nontoxic sodium heptanoate of formula $CH_3(CH_2)_5COONa$, noted NaC_7, on zinc corrosion. Electrochemical measurements have shown that the formation of the protective film is dependent on the heptanoate concentration and creates an efficient barrier against aggressive anions. According to investigations on the surface film, the protective material is a layered zinc hydroxyheptanoate $Zn_5(CH_3(CH_2)_5COO)_2(OH)_8$. Subsequent powder synthesis, thermogravimetric, and powder XRD analysis allowed us to propose a crystallographic model describing the structure of this protective coating as based on a hydrozincite one. The intercalation of organic anions in zinc layered metallic hydroxide may be an interesting way to block the deleterious incorporation of water and corrosive anions as chlorides in the interlayer space.

Introduction

Zinc is one of the most widely used metals especially in galvanized steel parts, and the atmospheric corrosion is the most prevalent type of damage of this metal.[1] Among the atmospheric corrosion forms of zinc, the "wet storage stain" occurring on galvanized steel surfaces during transport or storage can seriously affect the aspect and the qualities of zinc because of the formation of extensive white corrosion products, commonly called "white rust".[2,3] Indeed, the appearance of the "white rust" is promoted by the close packing of galvanized articles in humid medium. In confined environment, the moisture, resulting from direct exposure to rain, condensation, and/or incomplete drying after quenching can be retained by capillary action between the metallic parts in close packing. The local diffusion of oxygen in these microenvironments between two metallic parts induces a local attack of the metal surface by a differential aeration between the external surface and the interstice. Then, the zinc oxidation provokes the formation of white zinc based corrosion products on the surface, mainly composed by zinc layered hydroxide: $Zn_5Cl_2(OH)_8$, H_2O, and $Zn_5(CO_3)_2(OH)_6$.[4,5] The crystallization of these materials results in voluminous and powdery deposits on surfaces. Their crystallographic structures are lamellar and consist of a sheet stacking of zinc cations in octahedral and tetrahedral coordination of oxygen and hydroxyl anions, $[Zn_5(OH)_8]^{2+}$. These materials on zinc surfaces are susceptible to absorb chloride and water by exchange reactions or dissolution/coprecipitation mechanisms and constitute tanks to retain and maintain the humidity and the corrosive anions as chlorides.

In practice, applications of mineral oil or chromate coatings are used in the galvanizing industry as a surface treatment to prevent this phenomenon.[6] Nowadays, the imperative respect of environmental rules concerning wastewater rejects implies the development of effective, low-cost, and environmentally friendly anticorrosion treatment as alternatives to the current formulations based on chromate or mineral oil. Several anionic compounds, more or less toxic, have been investigated to fulfill this requirement: phosphates,[7−9] phosphonates, benzoates, and amine derivatives.[10−14]

Over the past 10 years, the efficiency of nontoxic linear sodium monocarboxylates of general formula $CH_3(CH_2)_{n-2}COONa$ as corrosion inhibitors of Cu, Fe, Pb, and Mg in aerated aqueous solutions was investigated.[15−18] As proved

* To whom correspondence should be addressed. E-mail: emmanuel.rocca@lcsm.uhp-nancy.fr.

(1) Zhang, G. X. *Corrosion and Electrochemistry of Zinc*; Plenum Press: New York, 1996.
(2) Gilbert, P. T.; Hadden, S. E. *J. Inst. Met.* **1950**, *78*, 47.
(3) Bird, C. E.; Strauss, F. J. *Mater. Perform.* **1976**, *15*, 27.
(4) Zhu, F.; Peerson, D.; Thierry, D. *Corrosion* **2001**, *57*, 582.
(5) Peerson, D.; Mikailov, A.; Thierry, D. Presented at Eurocor 2004-Proceedings, Sep 12−16, 2004, Nice, France.
(6) El-Mallah, A. T.; Magd, M. R. G. A. *Met. Finish.* **1984**, *68*, 54.
(7) Kuznetsov, Y. I.; Podgornova, L. P. *Zashch. Met.* **1983**, *19*, 98.
(8) De Pauli, C. P.; Derosa, O. A. H.; Giordiano, M. C. *J. Electroanal. Chem.* **1978**, *86*, 335.
(9) Awad, S. A.; Kamel, Kh. M. *J. Electroanal. Chem.* **1970**, *24*, 217.
(10) Leroy, R. L. *Mater. Perform.* **1980**, *19*, 54.
(11) Manov, S.; Lamazouère, A. M.; Aries, L. *Corros. Sci.* **2000**, *42*, 1235.
(12) *12. Manov, S.; Noli, F.; Lamazouère, A. M.; Aries, L. J. Appl. Electrochem.* **1999**, *29*, 995.
(13) Müller, B.; Förster, I. *Corrosion* **1996**, *52*, 786.
(14) Wragg, J. L.; Chamberlain, J. E.; Chann, L.; White, H. W.; Sugama, F.; Manalis, S. *J. Appl. Polym. Sci.* **1993**, *50*, 917.
(15) Rapin, C.; Steinmetz, P.; Steinmetz, J. *Corrosion (San Diego)* **1998**, *98*, C211.
(16) Hefter, G. T.; North, N. A.; Tan, S. H. *Corrosion* **1997**, *53*, 657.

10.1021/cm0616026 CCC: $33.50
Published on Web 12/01/2006

by XRD, IR, and XPS measurements, this kind of carboxylate has the ability to form a thin film of metallic soap after an initial oxidation of the metal surface by the dissolved oxygen in the treatment solution.[19] Usually, the material responsible of the corrosion protection on the metal has the general formula $M(CH_3(CH_2)_{n-2}COO)_2{\cdot}yH_2O$, where the cation is M^{2+}, n is the carbon number of the carboxylate anions, and y is the water content. Generally, the metallic soap is completely dehydrated with $y = 0$ except for magnesium soap.

The aim of this study is to develop a new protective material on zinc surface against corrosion by oxygen in moist environment. This new material should be present in a thin layer on the surface, should not contain toxic compounds such as chromium(VI), and should not have a greasy aspect on the metal surface. This study is focused on the action of sodium heptanoate of formula $CH_3(CH_2)_5COONa$, noted NaC_7, on the zinc surface in neutral and aerated solutions. In a first step, the evolution of the protection efficiency of NaC_7 solution as a function of its concentration was studied in an aerated reference corrosive medium at pH = 8 by using stationary electrochemical methods and electrochemical impedance spectroscopy (EIS). Then, the passivation of the zinc surface by a thin crystallized layer was demonstrated by scanning electron microscopy (SEM), X-ray diffraction (XRD), and infrared spectroscopy analyses. pH-controlled synthesis of the different materials precipitated from the Zn^{2+}/C_7 melt and their analysis allowed us to characterize the material responsible of the zinc protection in these conditions. Finally, thermal gravimetric analysis (TG) and XRD powder analysis permitted us to propose a structure model from an original metal hydroxide able to delay the corrosion phenomenon.

Experimental Section

The solutions of linear sodium heptanoate ($CH_3(CH_2)_5COONa$ or NaC_7) were prepared via neutralization of heptanoic acid (99%, Aldrich) by sodium hydroxide. The syntheses of the different powders of zinc soaps were performed by precipitation with help of a titration apparatus (721 NET Titrino Metrohm) driven by a computer. They were performed by adding, under stirring and nitrogen bubbling, 14 μL of a 0.1 mol·L^{-1} NaOH solution every 100 s into a $Zn(ClO_4)_2/HC_7$ melt (ratio $Zn/HC_7 = 1/2$) until the desired pH was reached. The initial pH of the mixing was adjusted to 2.5 with $HClO_4$ concentrated solution and 0.1 mol·L^{-1} $NaClO_4$ solution was used as ionic buffer. Then, the different white precipitates were filtered, rinsed with distilled water, and dried under vacuum in a desiccator. Thermal gravimetric analyses (TG: Setaram TG-DTA92-16 apparatus) were performed on synthesized compounds which were heated at 50 °C for 6 h to remove the surface water of the crystals and then from 50 to 500 °C with a heating rate of 1 °C·min^{-1} under argon flux.

For electrochemical experiments, the corrosive medium used as reference was the ASTM D 1384-87 standard[20] (noted afterward as ASTM water) with the following composition: 148 mg·L^{-1} Na_2SO_4; 138 mg·L^{-1} $NaHCO_3$; 165 mg·L^{-1} NaCl. Heptanoate solutions, ranging from 10^{-3} to 10^{-1} mol·L^{-1}, were made in ASTM medium, and their pH was adjusted to 8 by adding a NaOH solution. All the solutions prepared by this way were transparent and colorless without any insoluble acidic soap compounds.[21]

Electrochemical tests were performed, in aerated conditions, using a three-electrode electrochemical cell. The circular working electrode surface (0.283 cm^2) was vertical, facing the Pt-disk used as the counter electrode, and the reference electrode was a KCl-saturated calomel electrode (Hg/Hg_2Cl_2, $E = +0.242$ V/SHE). All the working electrode potentials were given versus this reference. The working electrode was pure zinc (99.9 wt % from Goodfellow). Before the experiments, the working electrode was mechanically polished with successively finer grades of SiC emery papers up to 1200 and then rinsed with distilled water and ethanol and dried. This device is connected to an EGG PAR 273A potentiostat driven by a computer equipped with the SoftCorr PAR software for data acquisition and analysis. The following experimental sequence was used:

(i) Measurement were made of corrosion potential (E_{cor}) and polarization resistance (R_p) every 1 h for a duration of 24 h, with a scan rate of 0.166 mV·s^{-1} for a range of 20 mV ($E_{cor} \pm 10$ mV). The error on the R_p assessment was evaluated at less than 10%.

(ii) Then there was recording of the potentiodynamic curve, $I = f(E)$, from −150 mV versus E_{cor} to 1200 mV, with a sweep rate of 1 mV·s^{-1}.

Electrochemical impedance spectroscopy experiments (EIS) were carried out with a Solartron 1255 FRA from 10^5 Hz to 10^{-1} Hz with a 10 mV amplitude, and the impedance data were fitted with Zsimpwin software using nonlinear least-squares fit techniques.[22]

The morphology of the protective layer formed on the zinc surface after immersion in a 0.1 mol·L^{-1} NaC_7 was observed by SEM (Hitachi S-2500 apparatus).

The surface layers were analyzed by X-ray diffraction (PHILIPS X'Pert PRO diffractometer) using copper Kα radiation ($d = 1.5418$ Å) and by infrared spectroscopy (FTIR Perkin-Elmer 2000 spectrometer) and then compared to synthesized powders. The IR measurements were conducted in diffuse reflection mode for the powders or with IRRAS configuration for surface analysis of the zinc substrate.

Results

(1) Electrochemical Study and Surface Analysis of Zinc in ASTM Water Containing NaC_7. The effect of heptanoate concentration and immersion time on the corrosion potential of zinc is shown in the Figure 1 and compared to that obtained in the NaC_7-free ASTM water. As it can be seen, the corrosion potential of zinc increases from the addition of 5×10^{-2} mol·L^{-1} NaC_7. This potential increase is about 500 mV with the addition of 0.1 mol·L^{-1} NaC_7 to ASTM water, which reveals a strong modification of the zinc surface in contact with heptanoate. It is interesting to note that the maximum E_{cor} value is rapidly reached and remains almost constant during the 24 h of the experiments, meaning that the zinc surface is modified in a short time of immersion. These high values of the corrosion potential seem to prove the presence of a thin layer, getting the metal nobler and then inhibiting the anodic reaction of the corrosion process.

(17) Rocca, E.; Steinmetz, J. *Corros. Sci.* **2001**, *43*, 891.
(18) Daloz, D.; Rapin, C.; Steinmetz, P.; Michot, G. *Corrosion* **1998**, *54*, 444.
(19) Rocca, E.; Bertrand, G.; Rapin, C.; Labrune, J. C. *J. Electroanal. Chem.* **2001**, *503*, 133.
(20) ASTM Standard D 1384-87: *Standard test method for corrosion test engine coolants in glassware*; ASTM: West Conshohocken, PA, 1988.
(21) Ekwall, P.; Fontell, K. *Colloid Polym. Sci.* **1988**, *266*, 184.
(22) Boukamp, B. A. *Solid State Ionics* **1986**, *20*, 31.

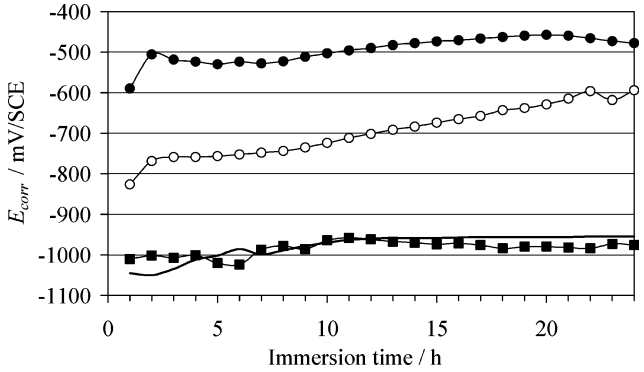

Figure 1. Corrosion potential E_{cor} of zinc versus immersion time in free-NaC_7 ASTM water (—) and ASTM water with NaC_7: 10^{-3} mol·L^{-1} (■); 5×10^{-2} mol·L^{-1} (○); 10^{-1} mol·L^{-1} (●).

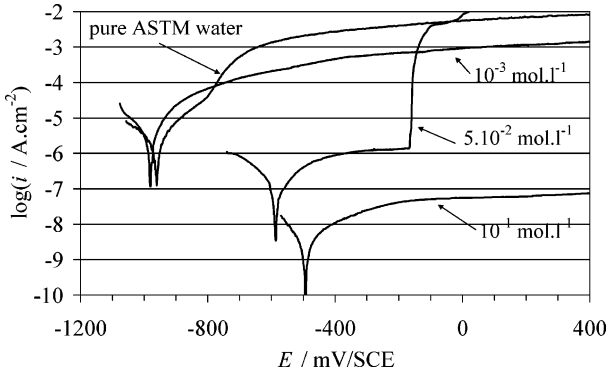

Figure 2. Potentiodynamic curves of zinc in free-NaC_7 ASTM water and in ASTM water containing 10^{-3} mol·L^{-1}, 5×10^{-2} mol·L^{-1}, or 10^{-1} mol·L^{-1} NaC_7 after 24 h of immersion.

The electrochemical behavior of zinc after 24 h of immersion in ASTM water with or without NaC_7 is displayed in Figure 2. The comparison of the potentiodynamic curves reveals that the addition of NaC_7 induces a strong decrease of the anodic current. In the absence of inhibitor or with 10^{-3} mol·L^{-1} NaC_7 solution, the anodic current density measured at -0.2 V is close to 10^{-3} A·cm^{-2} and corresponds to a rapid dissolution of zinc in Zn^{2+} cations in the ASTM water. When the NaC_7 concentration increases above 10^{-2} mol·L^{-1}, the current density at -0.2 V decreases sharply to a value of 14×10^{-8} A·cm^{-2} for 10^{-1} mol·L^{-1} NaC_7, which indicates that the pitting corrosion can be totally suppressed at high content of NaC_7. These results emphasize that the more the concentration is raised, the more the corrosion potential E_{cor} increases, from -0.96 V in NaC_7-free ASTM water to -0.5 V for 10^{-1} mol·L^{-1} NaC_7 solution. As supposed with the E_{cor} value, the presence of the thin protective layer mainly affects the kinetic of the anodic process of zinc corrosion by a large current decrease; the Tafel straight of the cathodic process is almost unchanged.

After immersion for 48 h in solution containing 10^{-1} mol·L^{-1} of NaC_7 at pH = 8, the zinc surfaces were observed by SEM. Some typical images are displayed in Figure 3 and reveal that the zinc surface is well-covered by a thin layer of a protective material (Figure 3a). Existence of a passive layer was clearly evidenced on the Figure 3b: the protective film was peeled off after immersion in liquid nitrogen.

According to the IR spectroscopy measurements displayed in the Figure 4, carboxylate species are present in the surface layer, as it is attested by the two peaks at 1550 cm^{-1} and

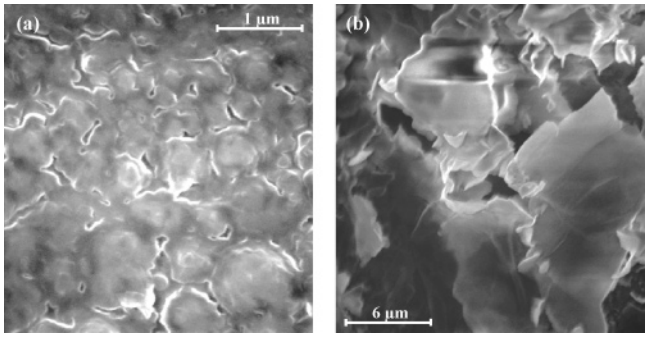

Figure 3. SEM micrographs of zinc surface treated by 10^{-1} mol·L^{-1} NaC_7 solution for 48 h (a) and protective layer peeled off after sample fracturing in liquid nitrogen (b).

1400 cm^{-1}, which are characteristics of the stretching frequencies of the COO^- group (respectively ν_a and ν_s), and by those around 2900 cm^{-1}, assigned to the stretching frequencies of CH_2 and CH_3 groups.[23] Moreover, this spectrum highlights the presence of hydroxyl groups OH^- in the protective layer by the occurrence of a specific large peak around 3400 cm^{-1} [23] (Figure 4a). On the other hand, the absence of the vibration around 1600 cm^{-1} characteristic of HOH bending indicates that the layer does not contain H_2O molecules.

The XRD measurements performed on the layer show the presence of a crystallized material with three peaks at low angles, characteristic of a layered compound as illustrated by periodic diffraction peaks (Figure 5).

To better characterize the protective behavior of this film on zinc, EIS spectra was recorded after 2 h of immersion of the substrate in ASTM water with or without NaC_7 (Figure 6). To interpret these results, the zinc surface was simulated by electrical equivalent circuits plotted in Figure 7. At pH = 5, the inductive loop at high frequency was not fitted. The choice of these circuits was a compromise between a reasonable fitting of the experiment values and a good description of the electrochemical system by keeping the number of circuit elements at a minimum.

In the ASTM and ASTM containing NaC_7 10^{-2} mol·L^{-1}, the zinc surface can be modeled by the electrolyte resistance, R_e, and two capacitive loops: the former is assigned to the electron transfer across the interface with a double layer capacity (CPE_{dl} − constant phase element − $1/Z = CPE_{dl}(j\omega)^n$) and a transfer resistance, R_t, and the latter is attributed to the oxygen diffusion near the interface, Z_d. This diffusion impedance Z_d related to the oxygen diffusion process in a finite region is characterized by two parameters: Y_0 and B. The equation for the complex impedance $Z_d(\omega)$ is given by the following: $Z_d(\omega) = \{1/Y_0\sqrt{j\omega}\}\tanh[B\sqrt{j\omega}]$. According to previous works,[24,25] the ratio B/Y_0 has a dimension of resistance (Ω) and can be assigned to the diffusion resistance of the specie ($R_d = B/Y_0$).

The numerical data relevant to the EIS fits summarized in Table 1 reveal that the addition of 10^{-2} mol·L^{-1} NaC_7

(23) Nakamoto, K. *Infrared and Raman Spectra of Inorganic and Coordination Compounds*, 5th ed.; John Wiley & Sons: New York, 1997.
(24) Macdonald, J. R. *Impedance spectroscopy-Emphasizing solid materials and systems*; John Wiley & Sons Inc.: New York, 1987.
(25) Franceschetti, D. R.; Macdonald, J. R. *J. Electroanal. Chem.* **1979**, *100*, 583.

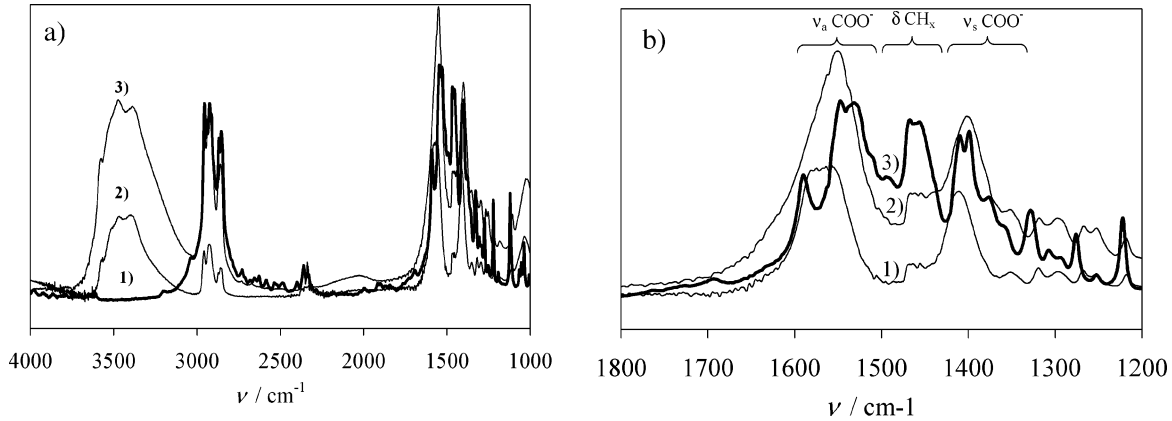

Figure 4. (a) IR spectra of $Zn(C_7)_2$ powder synthesized at pH = 5 (1), zinc surface treated by 10^{-1} mol·L^{-1} NaC_7 solution at pH = 8 for 48 h (2), and powder synthesized from Zn^{2+}/C_7 melt at pH = 8 (3). (b) Zoom in the 1200−1800 cm^{-1} range.

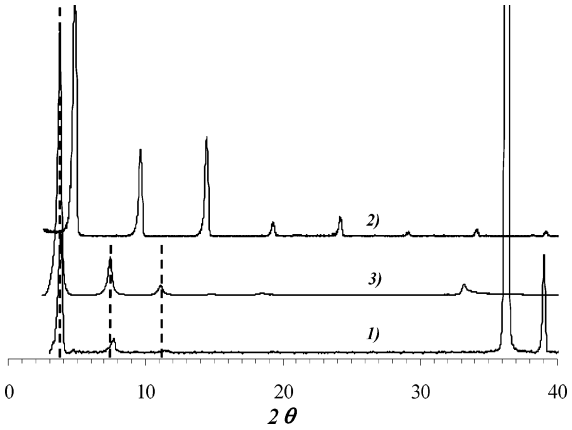

Figure 5. XRD patterns of passive layer treated by 10^{-1} mol·L^{-1} NaC_7 solution for 14 days (1), $Zn(C_7)_2$ powder synthesized at pH = 5 (2), and zinc hydroxyheptanoate $Zn(C_7)_{2-x}(OH)_x$ synthesized at pH = 8 (3).

does not change significantly the corrosion behavior of zinc. Indeed, the electron-transfer resistance R_t slightly increases, but the diffusion resistance R_d in the two cases remains around 10^4 Ω·cm^2. Moreover, the CPE_{dl} is almost constant which reveals the presence of a similar layer on the metal surface. These results confirm that 10^{-2} mol·L^{-1} NaC_7 in solution is not sufficient to build a thin layer able to efficiently protect the zinc surface.

In contrast, the impedance data of zinc surface in contact with 10^{-1} mol·L^{-1} NaC_7 highlight a much more capacitive and resistive behavior than the previous cases (Figure 6c). According to EIS fit (Table 1) obtained from electrical equivalent circuit displayed in Figure 7b, this behavior is clearly due to the presence of a thin layer having a very low capacity and a high resistance (C_{film}, R_{film}). In addition, the high value of diffusion resistance ($R_d = 5 \times 10^8$ Ω·cm^2) show that this material has the property to slow down the dissolution of zinc metal.

(2) Synthesis and Analysis of the Different Zn^{2+}/C_7-Based Materials. The zinc passivation is clearly due to the precipitation of a hydrophobic material constituted by heptanoate anions. To determine the different chemical compounds formed with Zn^{2+} and C_7^- anion, the pH of this mixture was monitored along a slow addition of NaOH in water solvent. Typical pH = f(V_{NaOH}) titration curves of the Zn^{2+} solutions without and with HC_7 are displayed in Figure 8. The curve of the pure Zn^{2+} solution shows one pH plateau corresponding in these conditions to the precipitation of zinc hydroxide at pH = 7.5. However, the curve obtained in the presence of C_7^- reveals two distinctive pH plateaus, which demonstrate there is precipitation of two successive compounds versus pH: the precipitation of the first one occurs around pH = 4.5 and the second one is detected at pH = 7.5. The final step at pH = 12 corresponds to the dissolution of the Zn^{2+}-based compounds into zincate ions (ZnO_2^-). Subsequently, the two different materials were synthesized at fixed pH: pH = 5 and pH = 8.

Synthesis at pH = 5. At pH = 5, the XRD pattern of the synthesized white powder corresponds to the one of zinc heptanoate, $Zn(C_7)_2$, which has a lamellar structure with a basal distance d = 18.5 Å (Figure 5, diffractogram 2). The crystallographic structure of $Zn(C_7)_2$ was determined in a previous study.[26,27]

The thermogravimetric curve of the $Zn(C_7)_2$ powder displayed in Figure 9 shows a weight loss around 300 °C, which corresponds to the decomposition of the heptanoate molecule leading to the formation of ZnO above 400 °C, as it has been proved by XRD analysis. Moreover, the absence of weight loss at low temperature and OH vibrations on IR spectrum confirms that zinc heptanoate does not contain hydroxyl or water in its crystallographic structure (Figure 4). Besides, according to the weight loss at 350 °C and the ZnO mass recovered at 500 °C, the stoichiometry of the $Zn(C_7)_2$ compound was verified.

Synthesis at pH = 8. The XRD pattern of the powder precipitated at pH = 8 displayed in the Figure 5 brings to light the presence of diffraction peaks different from $Zn(C_7)_2$ corresponding to another material. These new compound has also a lamellar structure characterized by a parameter of 23 Å larger than the one of $Zn(C_7)_2$ compound but similar to the one observed in the passive layer formed on zinc surface after immersion in NaC_7 solution at pH = 8 (Figure 5). The IR spectrum of the compound synthesized at pH = 8 is comparable to the one of the material constituting the passive layer on zinc (Figure 4). Indeed, the presence of carboxylate anions is characterized by the vibration of CH_2, CH_3, and COO groups. Hydroxide species characterized by the vibra-

(26) Peultier, J.; Rocca, E.; Steinmetz, J. *Corros. Sci.* **2003**, *45*, 1703.
(27) Peultier, J.; François, M.; Steinmetz, J. *Acta Crystallogr.* **1999**, *C55*, 2064.

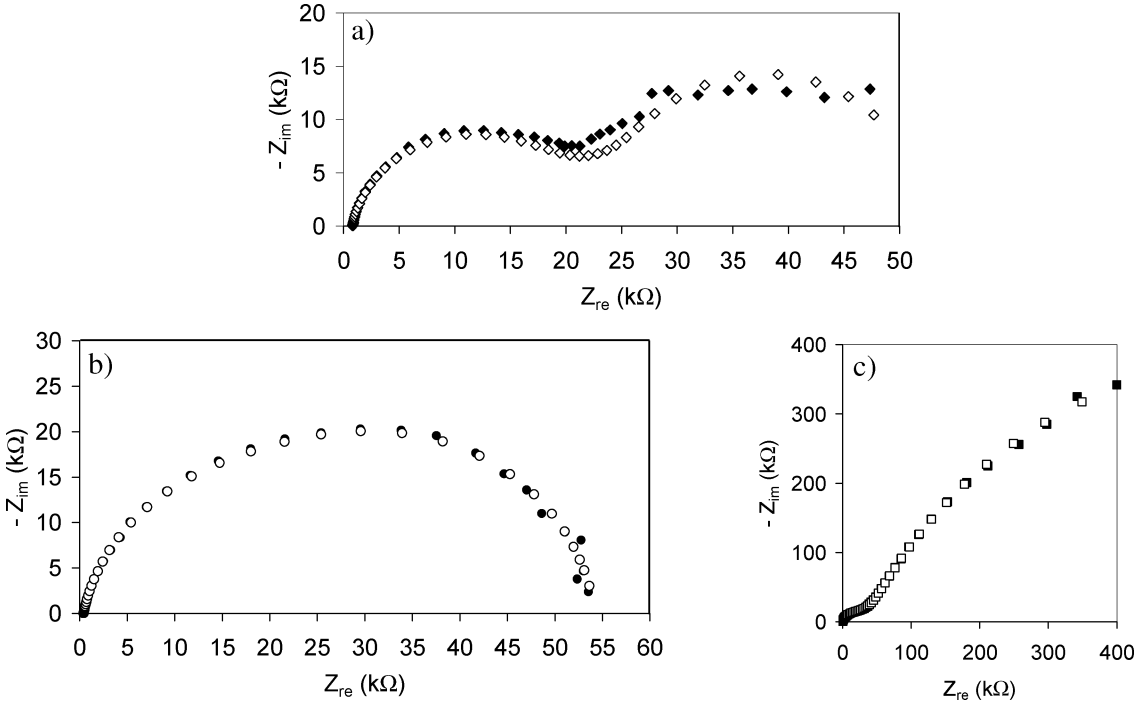

Figure 6. EIS spectra of zinc after 2 h of immersion in (a) ASTM water, (b) ASTM water with 10^{-2} mol·L^{-1} of NaC_7, and (c) ASTM water with 10^{-1} mol·L^{-1} of NaC_7. Data are represented by black symbols, and fit results by white ones.

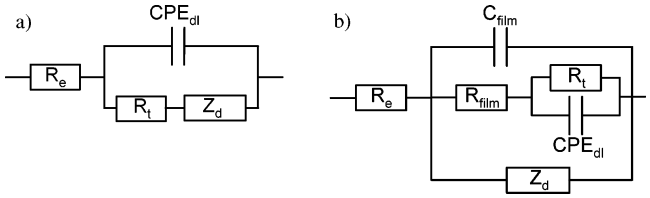

Figure 7. Electrical equivalent circuit used to fit the EIS data for Figure 6a (ASTM water) and Figure 6b (ASTM water + 0.01 M NaC_7) (a) and the EIS data for Figure 6c (ASTM water + 0.1 M NaC_7) (b).

tion at 3400 cm^{-1} are also identified in the structure but no water molecules (absence of peak around 1600 cm^{-1}).[23] Contrary to the thermogravimetric data of $Zn(C_7)_2$, the behavior of the compound at pH = 8 shows clearly a first weight loss at around 90 °C and the weight loss at 300 °C similar to the one observed during the decomposition of $Zn(C_7)_2$ and attributed to the decomposition of the heptanoate molecule (Figure 9). The weight loss occurring at 90 °C is ascribed to the removal of hydroxide groups from the structure, leading to the decomposition of the materials structure into ZnO beyond 150 °C, as proved by the XRD diffractogram versus temperature (Figure 10).

These TG and IR spectroscopy results prove the presence of both OH^- and C_7^- anions in the structure of the material precipitated at pH = 8. Further DSC experiments performed at low temperatures (50 to −30 °C) display no freezing peak, which confirms as well the absence of intercalated water in the structure.

Thus, a general formula can be proposed: $Zn(C_7)_{2-x}(OH)_x$ with $0 < x < 2$. Considering the global weight loss at 500 °C, the ZnO mass recovered at 500 °C, and the electroneutrality of the compound, the value of x can be evaluated to 1.51, which is closed to the most common formula of layered zinc hydroxide salts.

On the other hand, according to the pH-controlled titration of the Zn^{2+}/HC_7 melt (Figure 8), an addition of 2 mol of OH^- is necessary to completely precipitate $Zn(C_7)_2$ during the first plateau (pH = 4.5) according to the reaction

$$Zn^{2+} + 2HC_7 + 2NaOH \rightarrow Zn(C_7)_2(s) + 2Na^+ + 2H_2O$$

Then, a further addition of about 1.64 mol of OH^- was necessary to completely transform the $Zn(C_7)_2$ solid into $Zn(C_7)_{2-x}(OH)_x$ solid during the second plateau (pH = 7.5) according to the reaction

$$Zn(C_7)_2(s) + xNaOH \rightarrow Zn(C_7)_{2-x}(OH)_x(s) + xNaC_7$$

The average of the x value calculated from two kinds of experiment (TG and pH-controlled titration) is 1.57, leading to a stoichiometry of the hydroxyhaptanoate of zinc, $Zn(C_7)_{0.43}(OH)_{1.57}$. Elementary analysis of the compound carried out in Service Central d'Analyze at Vernaison, France, by ICP-AES confirm this stoichiometry (Zn, 45 wt %; C, 23 wt %; O, 27 wt %).

A model for $Zn_5(C_7)_2(OH)_8$ extrapolated from the hydrozincite structure $Zn_5(CO_3)_2(OH)_6$ was refined using the powder XRD data.[28] The orientation of the heptanoate chains was found in a monoclinic $P2$ lattice with parameters a = 23.092(4) Å, b = 6.250(4) Å, c = 5.421(6) Å, and β = 95.63(1)°, using the Fox program.[29] Then the structure was refined using Fullprof Suite[30] program (R_P = 0.12, R_{WP} = 0.15, R_B = 0.12, χ^2 = 9.18). The observed, calculated, and difference patterns are represented in Figure 11a. A graphic representation and some selected interatomic distances are reported in the Figure 11b and Table 2 respectively.

(28) *Ghose, S. Acta Crystallogr.* **1964**, *17*, 1051.
(29) Favre-Nicolin, V.; Cerny, R. J. Appl. Crystallogr. **2002**, *35*, 734.
(30) Rodriguez-Carvajal, J. *FULLPROF*, version June 2005, ILL.

Table 1. Value of Electrical Elements of Equivalent Circuit Fitting of the EIS Data of Figure 6

ASTM water		ASTM water + 0.01 M NaC_7		ASTM water + 0.1 M NaC_7	
R_e (Ω•cm^2)	810	R_e (Ω•cm^2)	413	R_e (Ω•cm^2)	152
CPE_{film} (μF•cm^2)	2.8	CPE_{film} (μF•cm^2)	2.5	C_{film} (μF•cm^2)	0.025
n	0.88	n	0.88	R_{film} (Ω•cm^2)	1.71×10^6
R_t (Ω•cm^2)	18 900	R_t (Ω•cm^2)	36 400	CPE_{dl} (μF•cm^2)	1.89
$Z_d - Y_0$	1.1×10^{-4}	$Z_d - Y_0$	3.5×10^{-5}	n	0.71
$Z_d - B$ ($s^{0.5}$)	3.62	$Z_d - B$ ($s^{0.5}$)	0.62	R_t (Ω•cm^2)	51 100
				$Z_d - Y_0$	9.5×10^{-7}
				$Z_d - B$ ($s^{0.5}$)	478

Discussion

From the results obtained through this study, the hydroxyheptanoate thin layer formed on zinc can be an efficient solution for inhibiting the zinc corrosion.

Electrochemical characterizations reveal clearly that the C_7-based layer slows down drastically the rate of the anodic reaction of the zinc corrosion, as shown by the strong decrease of the anodic current and by the anodic shift of the corrosion potential in presence of NaC_7. According to EIS analyze, the protective character of the C_7-based layer is due to the high resistance and low capacity of the material forming the film, which also acts as a very effective barrier against the dissolution of zinc metal.

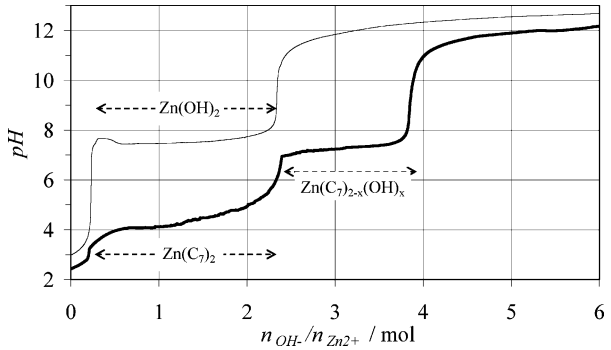

Figure 8. Titration of Zn^{2+} solution without (thin line) and with HC_7 (bold line) as a function of pH (Zn^{2+}/HC_7: 1/2 in moles) with NaOH solution.

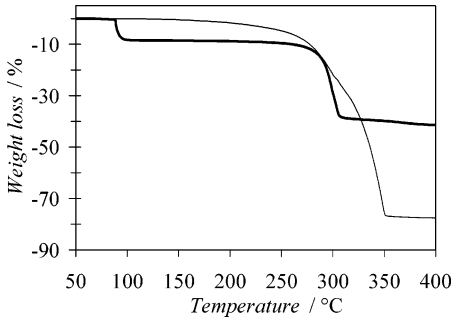

Figure 9. Thermogravimetric analysis (TG) of zinc heptanoate $Zn(C_7)_2$ (synthesized at pH = 5) with a thin line and zinc hydroxyheptanoate $Zn(C_7)_{2-x}(OH)_x$ with a bold line (synthesized at pH = 8)

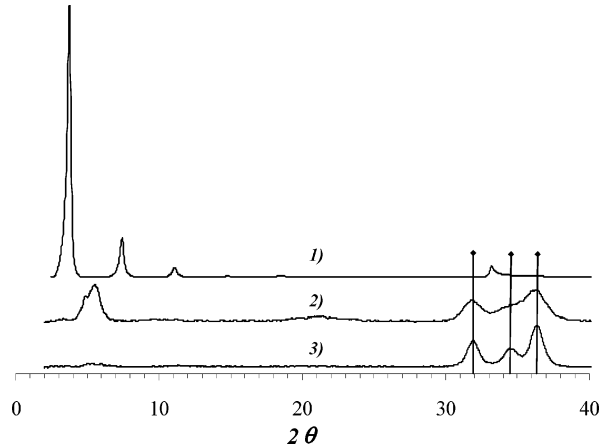

Figure 10. XRD patterns of $Zn(C_7)_{2-x}(OH)_x$ (synthesized at pH = 8) at 20 °C (1) and after thermogravimetric experiments stopped at 150 °C (2) and 500 °C (3). Key: ■, ZnO peaks.

A simple mechanism of film formation on zinc can be proposed in Figure 12: after an initial oxidation of zinc into Zn^{2+} cations by the oxygen dissolved in the solution, a thin protective layer is formed on the metal by coprecipitation of a heptanoate-base zinc compound. According to the pH value, two different materials with Zn^{2+} and heptanoate anions can be precipitated. At low pH (around 5), the precipitation of zinc heptanoate $Zn(C_7)_2$ produce a thick and well-crystallized layer on zinc surface, as reported in previous study.[26] Then at neutral pH (around 8), the growth of a very thin film containing both hydroxyl and heptanoate anions was identified. The stoichiometry of this hydroxyheptanoate corresponds to the $Zn_5(CH_3(CH_2)_5COO)_2(OH)_8$ formulas.

This type of zinc layered hydroxide salts was already reported with chloride, nitrate, and others anions with a general stoichiometry of $Zn_5A_2(OH)_8$, where A is a monocharged anion.[31−34] The crystallographic model of these compounds can be considered as a variation of $Zn(OH)_2$ structure which is a close packing of sheets composed by zinc cations in octahedral coordination of hydroxyl anions. In these layered hydroxide salts, one-quarter of the zinc atoms in octahedral position are removed from the sheets and replaced by two zinc atoms in tetrahedral coordination of OH^- anions and water molecules. Thus, zinc ions in octahedral and tetrahedral coordination are in the 3:2 ratio in the sheets and the cohesion between the sheets is provided by van der Waals forces. To detail the charge distribution between the sheets and the anions, we can write a general formula

Two kinds of anions organization in the interlamellar space can be observed. In the structure of $Zn_5(NO_3)_2(OH)_8$•$2H_2O$[31] or $Zn_5(CH_3COO)_2(OH)_8$•$2H_2O$,[34] the tetrahedral fourth apex pointing in the interlamellar space is occupied by the oxygen of the water molecule and the anions are intercalated between the zinc sheets, whereas, in the $Zn_5Cl_2(OH)_8$•H_2O[32] and hydrozincite $Zn_5(CO_3)_2(OH)_6$[28] (without water), the anions occupy the fourth apex of the tetrahedron and the water molecules are intercalated in the interlamellar space.

(31) Stahln, W.; Oswald, H. R. *Acta Crystallogr.* **1970**, *B26*, 860.
(32) Allmann, R. Z. *Kristallogr.* **1968**, *126*, 417.
(33) Steven, S. P.; Jones, W. *J. Solid State Chem.* **1999**, *148*, 26.
(34) Poul, L.; Jouini, N.; Fievet, F. *Chem. Mater.* **2000**, *12*, 3123.

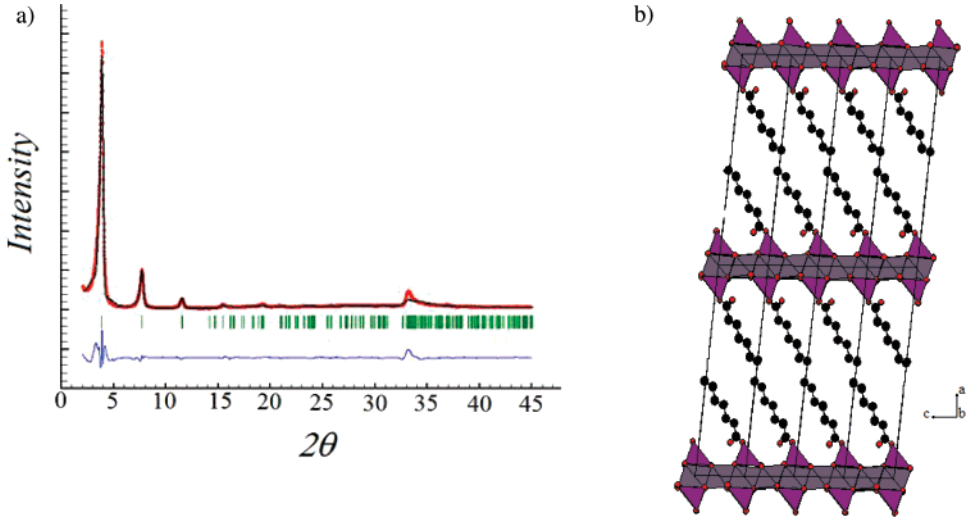

Figure 11. (a) Observed, calculated and difference XRPD patterns of $Zn_5(C_7)_2(OH)_8$. (b) Crystallographic model of zinc hydroxyheptanoate $Zn_5(C_7)_2(OH)_8$: carbon in black; ZnO_6 octahedron in gray; ZnO_4 tetrahedron in violet; oxygen of COO^- group in red.

Table 2. Selected Interatomic Distances (Å) in $Zn_5(C_7)_2(OH)_8$

Zn(1)−OH(1)	2.19(1)	Zn(3)−OH(1)	2 × 2.11(2)
Zn(1)−OH(2)	2.20(2)	Zn(3)−OH(3)	2 × 2.10(2)
Zn(1)−OH(3)	2.02(1)	Zn(3)−OH(4)	2 × 2.13(1)
Zn(1)−O(11)	1.97(1)	Zn(4)−OH(2)	2 × 2.12(1)
Zn(2)−OH(1)	2 × 2.12(1)	Zn(4)−OH(3)	2 × 2.10(2)
Zn(2)−OH(2)	2 × 2.10(1)	Zn(4)−OH(4)	2 × 2.01(1)
Zn(2)−OH(4)	2 × 2.11(1)		

In the case of zinc hydroxyheptanoate, the absence of peak around 1600 cm^{-1} (corresponding to the vibration of HOH molecules) points out that no water is involved in the structure. Consequently, the $CH_3(CH_2)_5COO^-$ anions should be directly bonded to the zinc sheets at the apex of tetrahedron. In addition, the contribution of an oxygen atom from the COO^- group to the coordination of zinc tetrahedron is confirmed by the COO^- stretching frequencies around 1500 cm^{-1}. Indeed, the values of the COO^- stretching frequencies of the zinc hydroxyheptanoate material are very close to those in the $Zn(C_7)_2$ material where the oxygens of COO^- groups are linked to Zn^{2+} cations in tetrahedral coordination.[27] In the case of reaction products of $Zn(OH)_2$ with organic compounds, Ogata et al. also suppose the transformation of $Zn(OH)_2$ sheet into a hydrozincite sheet to explain the stoichiometry of the formed organic−inorganic zinc salts.[36]

Consequently, a crystallographic model, $Zn_5(CH_3(CH_2)_5COO)_2(OH)_8$, based on hydrozincite structure can be set up to fit powder X-ray diffraction data. The sheets are build by $Zn(2)(OH)_6$, $Zn(3)(OH)_6$, and $Zn(4)(OH)_6$ octahedra linked by edges. The $Zn(1)(OH)_3O$ tetrahedra are located below and above the holes formed in the sheets (sheets 1.91 Å apart) as in the hydrozincite. The fourth O-coordination is ensured by O-atoms of the monodendate heptanoate chains with adjacent sheets of spacing 23.09 Å. van der Waals spacing is 2.32 Å.

Layered hydroxides and particularly double hydroxides were investigated for many years as host materials for a large range of intercalation or coprecipitation reactions[35,36] and were widely used as ion-exchange materials, catalysts, sorbents, etc. Many hydroxides in corrosion products have also layered structures which have the ability to absorb or exchange corrosive anions as chloride or sulfate.[1] In the $Zn_5(C_7)_2(OH)_8$ material, the intercalation of heptanoate anions stabilizes the hydrozincite sheets, which are the main crystallographic bricks constituting the zinc corrosion compounds. Thus, this avoids the water absorption in the structure and seems to block the exchange reaction with chloride or sulfate. Furthermore, the intercalation of a long carbon chain in the crystallographic structure explains the hydrophobic character of the layered material as shown by the Figure 13.

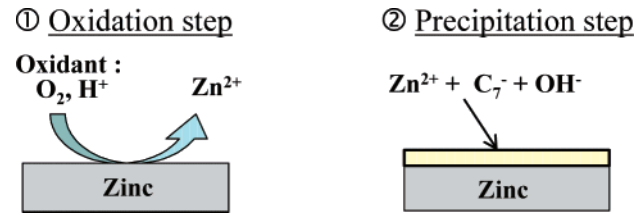

Figure 12. Two steps in the mechanism of formation of $Zn_5(C_7)_2(OH)_8$ on the zinc surface.

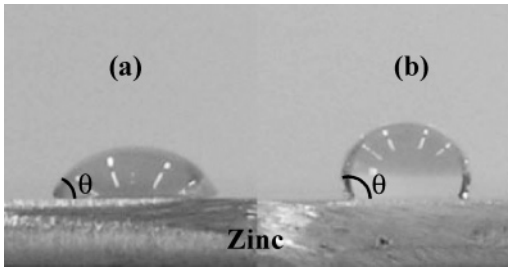

Figure 13. Shapes of water drops (V_{drop} = 50 μL) in contact with (a) a nontreated zinc surface and (b) a zinc surface inhibited in a 10^{-1} mol·L^{-1} NaC_7 aqueous solution at pH = 8 for 48 h.

Conclusion

Through this study, the intercalation of heptanoate anions in the layered zinc hydroxide has induced the stabilization of an organic−inorganic material, $Zn_5(CH_3(CH_2)_5COO)_2(OH)_8$, having interesting anticorrosion properties.

(35) Khan, A. I.; O'Hare, D *J. Mater. Chem.* **2002**, *12*, 3191.
(36) Ogata, S.; Miyazaki, I.; Tasaka, Y.; Tagaya, H.; Kadokawa, J.-I.; Chiba, K. *J. Mater. Chem.* **1998**, *8*, 2813.

Indeed, the immersion of zinc metal in oxygenated water solutions containing heptanoate anions easily leads to the growth of a thin layer of this material inhibiting the appearance of "white rust" on zinc in corrosive environment. So, by the combination of several analytical techniques, the same crystallographic sheet $[Zn_{1+x}(OH)_2]^{+2x}$ (with $x = 0.25$) as the materials constituting the "white rust" forms the crystallographic structure unit of $Zn_5(CH_3(CH_2)_5COO)_2(OH)_8$. Consequently, the intercalation of heptanotate between the hydrozincite sheets lead to a compact inorganic−organic material, which acts as a barrier material on zinc surface against oxidant as oxygen. Moreover, this compact and hydrophobic material avoids the absorption of chloride and water, which are the cause of the "white rust" growth. Finally, use of host structure of corrosion products to block their reactivity constitutes an interesting way to imagine new and environmentally friendly anticorrosion treatment.

CM0616026